Atmos. Meas. Tech. Discuss., 8, 1615–1627, 2015
www.atmos-meas-tech-discuss.net/8/1615/2015/
doi:10.5194/amtd-8-1615-2015

Atmospheric Measurement Techniques Discussions
Open Access

Electron density profiles probed by radio occultation of FORMOSAT-7/COSMIC-2 at 520 and 800 km altitude

J. Y. Liu[1,2,3], C. Y. Lin[1], and H. F. Tsai[4]

[1]Institute of Space Science, National Central University, Taoyuan, Taiwan
[2]Center for Space and Remote Sensing Research, National Central University, Taoyuan, Taiwan
[3]National Space Organization, Hsinchu, Taiwan
[4]Department of Earth Sciences, National Cheng Kung University, Tainan, Taiwan

Received: 1 November 2014 – Accepted: 20 January 2015 – Published: 4 February 2015

Correspondence to: J. Y. Liu (jyliu@jupiter.ss.ncu.edu.tw)

Published by Copernicus Publications on behalf of the European Geosciences Union.

Abstract

The FORMOSAT-7/COSMIC-2 (F7/C2) will ultimately place 12 satellites in orbit with two launches with 24° inclination and 520 km altitude in 2016 and with 72° inclination and 800 km altitude in 2019. In this study, we examine the electron density probed at the two satellite altitudes 500 and 800 km by means of FORMOSAT-3/COSMIC (F3/C) observations at the packing orbit 500 km altitude and mission orbit 800 km altitude, as well as observing system simulation experiments (OSSE). The electron density derived from 500 and 800 km satellite altitude of the F3/C observation and the OSSE confirm that the standard Abel inversion can correctly derive the electron density profile.

1 Introduction

On 15 April 2006, 6 micro-satellites of FORMOSAT-3/COSMIC (F3/C) were launched to the parking orbit of about 516 km and subsequently lifted to the mission orbit at 800 km, with inclination of 72°. Each micro satellite has been receiving the GPS signal to carry out radio occultation (RO), which yields abundant information about neutral atmospheric temperature and moisture as well as space weather estimates of slant total electron content (TEC), electron density profiles, and an amplitude scintillation index, S4 (Schreiner et al., 2007). The Abel inversion (cf. Hajj and Romans, 1998) has been employed to invert the electron density from the RO TEC. With the success of F3/C, the United States and Taiwan are moving forward with a follow-on RO mission named FORMOSAT-7/COSMIC-2 (F7/C2), which will ultimately place 12 satellites in orbit with two launches with 24° inclination and 520 km altitude in 2016 and with 72° inclination and 800 km altitude in 2019 (Lee et al., 2013; Yue et al., 2014). Scientists find that the local spherical symmetry assumption in the standard (Abel) RO inversion processes result in systemic biases, especially the EIA (equatorial ionization anomaly) at low latitudes, where the horizontal gradient is most significant (cf. Liu et al., 2010). Note that to conduct the Abel inversion, the electron density at the satellite altitude should be

AMTD

8, 1615–1627, 2015

Electron density profiles probed by radio occultation

J. Y. Liu et al.

assumed (Lei et al., 2007). However, Yue et al. (2011) evaluated of the effect of the orbit altitude electron on the Abel inversion from radio occultation measurements, and found no essential influence on the Abel retrieved electron density. In this paper, we examine the effect of satellite altitude on the Abel inversion by firstly comparing the electron density profiles ranging from 100 to 500 km altitude observed by satellites at 500 and 800 km altitude and their differences during the early F3/C mission period. Observing system simulation experiments (OSSEs) by means of the standard F3/C Abel inversion is used to produce above the observation. Cross comparisons among the observation and the OSSE shall have a better understanding on the electron density profiles observed at 520 and 800 km altitude for the upcoming F7/C2 mission.

2 F3/C electron density profiles observed at 500 and 800 km altitude

One half of F3/C satellites were orbiting at the parking orbit 500 km altitude and the other half at the mission orbit 800 km altitude in March and April 2007 (Fig. 1). The satellites at 500 and 800 km altitude probed 5812 and 5425 electron density profiles during 12:00–14:00 UT. The electron density profiles are gridded with 10° in latitude, 20° in longitude, and 10 km in altitude and the median of the electron density in each grid is computed. Figure 2 displays that the global electron density N, F2-peak electron density NmF2, and height hmF2 observed at the 500 and 800 km satellite altitude, and their difference. The longitude cuts in −120, −60, 0, 60, and 120° stand for the electron density at 05:00, 09:00, 13:00, 17:00, and 21:00 LT, respectively. It can be seen that structures of the electron density observed from 500 km satellite altitude (N_{500}) and from 800 km satellite altitude (N_{800}) at 09:00, 13:00, 17:00, and 21:00 LT are similar, respectively. Since the accuracy in the lower ionosphere is relatively low, we focus on the electron density in the topside ionosphere (i.e. the region above the F2-peak). It can be seen that the N_{500} is slightly greater (less) than N_{800} in the equatorial (off-equator) ionosphere, while N_{500} is slightly weaker than N_{800} in the South Pole region at 09:00 LT. N_{500} is greater than N_{800} in the EIA region at 13:00 LT; N_{500} is weaker

AMTD
8, 1615–1627, 2015

(greater) than N_{800} in the Northern (Southern) EIA region at 17:00 LT; and N_{500} is weaker than N_{800} in the Southern EIA region at 21:00 LT. The difference between the two electron densities N_{500}–N_{800} generally agree with the above comparisons, and also reveal that N_{500} is greater than N_{800} in the Northern EIA at 21:00 LT. The F2-peak electron density NmF2 observed from 500 and 800 km altitude (NmF2$_{500}$ and NmF2$_{800}$) displays that the two NmF2s yield similar patterns and NmF2$_{800}$ is generally greater than NmF2$_{500}$ in the Northern EIA area. However, due to the data locations being different, the difference of NmF2$_{500}$–NmF2$_{800}$ is difficult to identical. The F2-peak height hmF2 probed from 500 and 800 km satellite altitude (hmF2$_{500}$ and hmF2$_{800}$) as well as their difference illustrated that the two hmF2 are general similar in the low- and mid-latitude. In short, the F3/C electron densities observed from 500 and 800 km satellite altitude are qualitatively similar.

3 Abel OSSE

To carry out Abel OSSEs, we first insert realistic F3/C RO ray path geometries into the corresponding ionosphere computed by the IRI-2007 (Bilitza and Reinisch, 2008) to simulate the total electron content (TEC), and then apply the Abel inversion routine of CDAAC (COSMIC Data Analysis and Archival Center) to derive electron density profiles. Figure 3 displays the truth of the electron density, the NmF2, and hmF2 computed by IRI. The truth electron density shows that the EIA is greater in the Northern Hemisphere than that in the Southern, which can be fund in NmF2 distributions. The daytime hmF2 reaches the highest altitude in the EIA region, while hmF2 at mid- and high-latitudes in nighttime are higher than these in daytime. Figure 4 depicts OSSE electron density, NmF2, and hmF2 observed by satellites at 500 and 800 km altitude, and their difference. It can be seen that N_{500} is slightly weaker than N_{800} in the South Pole region at 09:00 LT; N_{500} is greater than N_{800} in the EIA region at 13:00 and 17:00 LT; and N_{500} is weaker than N_{800} in the Southern EIA region at 21:00 LT. Note that both N_{500} and N_{800} in EIA are greater in the Northern than these in the Southern obtained by the Abel

AMTD
8, 1615–1627, 2015
Electron density profiles probed by radio occultation
J. Y. Liu et al.

OSSE, which agree with the truth, respectively. It should be mention that the difference between N_{500} and N_{800} of the F3/C observation and that of the Abel OSSE yield similar features. The OSSE reveals that the $Nm\mathrm{F2}_{500}$ is slightly less than $Nm\mathrm{F2}_{800}$ in the Northern EIA region, and however the corresponding difference $Nm\mathrm{F2}_{500}$–$Nm\mathrm{F2}_{800}$ are rather complex. On the other hand, $hm\mathrm{F2}_{500}$ and $hm\mathrm{F2}_{800}$ in the low- and mid-latitudes are similar generally.

We further calculate the errors due to the different satellite altitudes of 500 and 800 km by subtracting the results of the Abel OSSE from the IRI truth. The error patterns between the two are accordingly similar that both N_{500} and N_{800} underestimate (overestimate) the electron density above (below) the F2-peak height (Fig. 5a and b). Again, we focus the topside ionosphere. The underestimation of N_{500} is more severe than that of N_{800} above F2-peak in the EIA region at 13:00 LT and N_{500} is not so severe as N_{800} above F2-peak in the EIA region at 09:00 LT and 17:00 LT. On the other hand, the error patterns of $Nm\mathrm{F2}_{500}$ and $Nm\mathrm{F2}_{800}$ are similar, which underestimate in the two EIA crests but overestimate in their poleward sides. It is interesting to find that the errors of both $hm\mathrm{F2}_{500}$ and $hm\mathrm{F2}_{800}$ are similar, which show hmF2 being mostly underestimated globally.

4 Discussion and conclusion

The F3/C observation and OSSE show that the electron density, NmF2, and hmF2 probed at 500 and 800 km altitude are similar (Figs. 2a and b and 4a and b). Although the real and IRI ionospheres might be different, the differences N_{500}–N_{800} shown in Figs. 2c and 4c are somewhat similar, especially in the topside ionosphere. Table 1 reveals that the overall difference N_{500}–N_{800} of the F3/C observation and OSSE are 23.5 ± 35.1 and 18.7 ± 26.6 %. Similarly, $Nm\mathrm{F2}_{500}$ and $Nm\mathrm{F2}_{800}$ as well as $hm\mathrm{F2}_{500}$ and $hm\mathrm{F2}_{800}$ of the F3/C observation and OSSE are nearly identical (Fig. 2d and e, Fig. 4d and e). Table 1 illustrates that the overall differences $Nm\mathrm{F2}_{500}$–$Nm\mathrm{F2}_{800}$ ($hm\mathrm{F2}_{500}$–$hm\mathrm{F2}_{800}$) of the F3/C observation and OSSE are 28.0 ± 39.1 and 19.4 ± 29.9 % (31.4 ±

AMTD
8, 1615–1627, 2015

55.1 and 27.0 ± 39.5 km), respectively. The similarities and the difference means being about and less 30 % imply that the Abel inversion routine of CDAAC can be applied to correctly derive electron density profiles by the RO TEC probed at 500 km satellite altitude. Figure 5 reveals the OSSE errors that the Abel inversion results in the topside ionospheric electron density and *hm*F2 being underestimated. Table 1 displays the OSSE errors of the electron density, *Nm*F2, and *hm*F2 at 500 and 800 km altitude are nearly identical, respectively. This suggests that the Abel inversion routine of CDAAC can be employed to correctly derive electron density profiles from the RO TEC sounded at 520 km F7/C2 satellite altitude.

Acknowledgements. This study is supported by the Taiwan Ministry of Science and Technology grant MOST 103-2628-M-008-001. The authors gratefully acknowledge the COSMIC Data Analysis and Archival Center (CDAAC) and Taiwan Analysis Center for COSMIC (TACC) for providing the FORMOSAT-3/COSMIC data.

References

Bilitza, D. and Reinisch, B.: International reference ionosphere 2007: improvements and new parameters, Adv. Space Res., 42, 599–609, doi:10.1016/j.asr.2007.07.048, 2008.

Hajj, G. A. and Romans, L. J.: Ionospheric electron density profiles obtained with the global positioning system: results from the GPS/MET experiment, Radio Sci., 33, 175–190, doi:10.1029/97RS03183, 1998.

Lee, I. T., Tsai, H. F., Liu, J. Y., Lin, C. H., Matsuo, T., and Chang, L. C.: Modeling impact of FORMOSAT-7/COSMIC-2 mission on ionospheric space weather monitoring, J. Geophys. Res.-Space, 118, 6518–6523, doi:10.1002/jgra.50538, 2013.

Lei, J., Syndergaard, S., Burns, A. G., Solomon, S. C., Wang, W., Zeng, Z., Roble, R. G., Wu, Q., Kuo, Y.-H., Holt, J. M., Zhang, S. R., Hysell, D. L., Rodrigues, F. S., and Lin, C. H.: Comparison of COSMIC ionospheric measurements with ground-based observations and model predictions: preliminary results, J. Geophys. Res., 112, A07308, doi:10.1029/2006JA012240, 2007.

Liu, J. Y., Lin, C. Y., Lin, C. H., Tsai, H. F., Solomon, S. C., Sun, Y. Y., Lee, I. T., Schreiner, W. S., Kuo, Y. H.: Artificial plasma cave in the low-latitude ionosphere results from the radio occultation inversion of the FORMOSAT-3/COSMIC, J. Geophys. Res., 115, A07319, doi:10.1029/2009JA015079, 2010.

Schreiner, W., Rocken, C., Sokolovskiy, S., Syndergaard, S., and Hunt, D.: Estimates of the precision of GPS radio occultations from the COSMIC/FORMOSAT-3 mission, Geophys. Res. Lett., 34, L04808, doi:10.1029/2006GL027557, 2007.

Yue, X., Schreiner, W. S., Rocken, C., and Kuo, Y.-H.: Evaluation of the orbit altitude electron density estimation and its effect on the Abel inversion from radio occultation measurements, Radio Sci., 46, RS1013, doi:10.1029/2010RS004514, 2011.

Yue, X., Schreiner, W. S., Pedatella, N., Anthes, R. A., Mannucci, A. J., Straus, P. R., and Liu, J. Y.: Space weather observations by GNSS radio occultationfrom FORMOSAT- 3/COSMIC to FORMOSAT-7/COSMIC-2, Space Weather, 12, 616–621, doi:10.1002/2014SW001133, 2014.

AMTD

8, 1615–1627, 2015

Electron density profiles probed by radio occultation

J. Y. Liu et al.

AMTD
8, 1615–1627, 2015

Electron density profiles probed by radio occultation

J. Y. Liu et al.

Table 1. The differences of N, NmF2, and hmF2 observed at 500 and 800 km altitude.

	F3/C 500–800 km	Abel OSSE 500–800 km	Abel OSSE 500 km–Truth	Abel OSSE 800 km–Truth
ΔN (%)	23.5 ± 35.1	18.7 ± 26.6	32.8 ± 46.8	31.3 ± 46.7
ΔNmF2 (%)	28.0 ± 39.1	19.4 ± 29.9	10.0 ± 13.0	11.0 ± 12.7
ΔhmF2 (km)	31.4 ± 55.1	27.0 ± 39.5	30.3 ± 28.5	32.0 ± 23.6

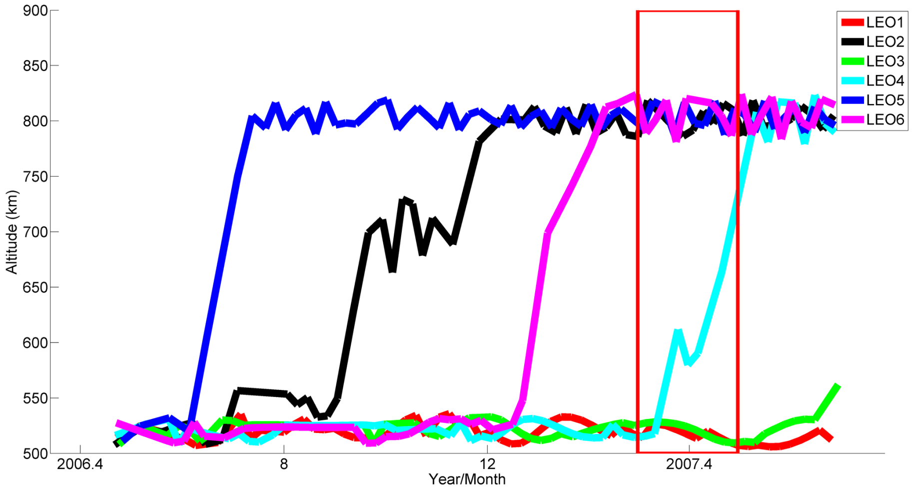

Figure 1. The altitude of each F3/C micro satellite from launched to middle of 2007. The red box indicates the time period of the study.

AMTD
8, 1615–1627, 2015

Electron density profiles probed by radio occultation

J. Y. Liu et al.

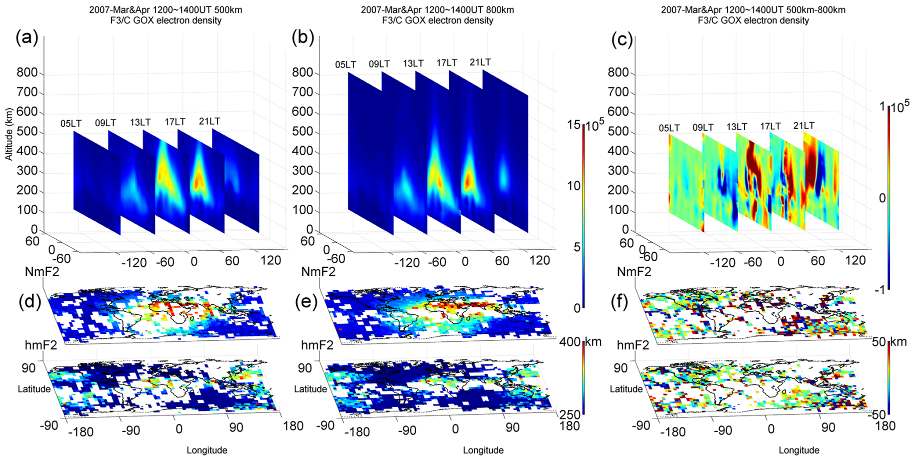

Figure 2. The F3/C electron density, *Nm*F2, and *hm*F2 observed from 500 and 800 km altitude satellites, and their difference during 12:00–14:00 UT in March and April 2007. **(a)** F3/C electron density observed from 500 km altitude, **(b)** F3/C electron density observed from 800 km altitude, and **(c)** their difference. **(d)** F3/C *Nm*F2 and *hm*F2 observed from 500 km altitude, **(e)** F3/C *Nm*F2 and *hm*F2 observed from 800 km altitude, and **(f)** their difference.

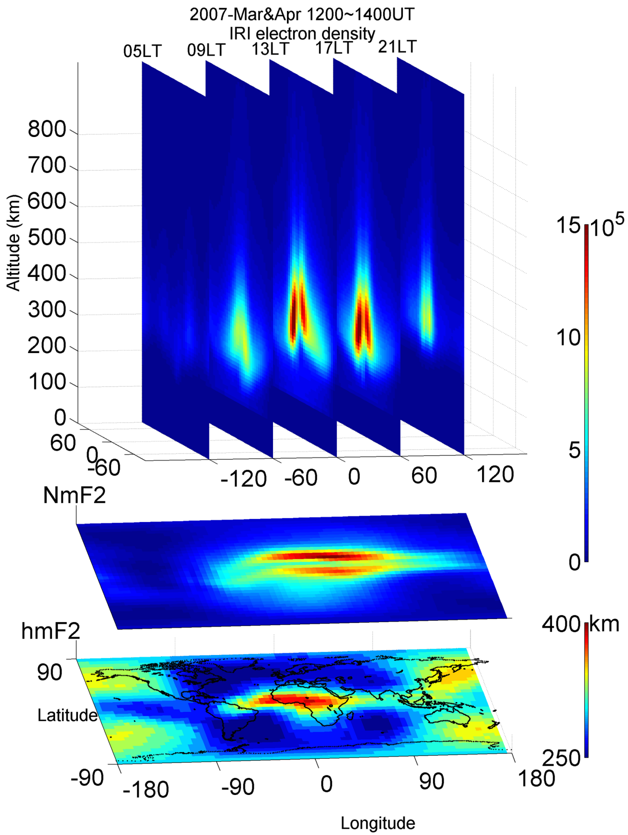

Figure 3. The OSSE Truth. The median of IRI output obtained from 12:00–14:00 UT in March and April 2007. The electron density distribution, *Nm*F2, and *hm*F2 are showed from up to down.

AMTD
8, 1615–1627, 2015

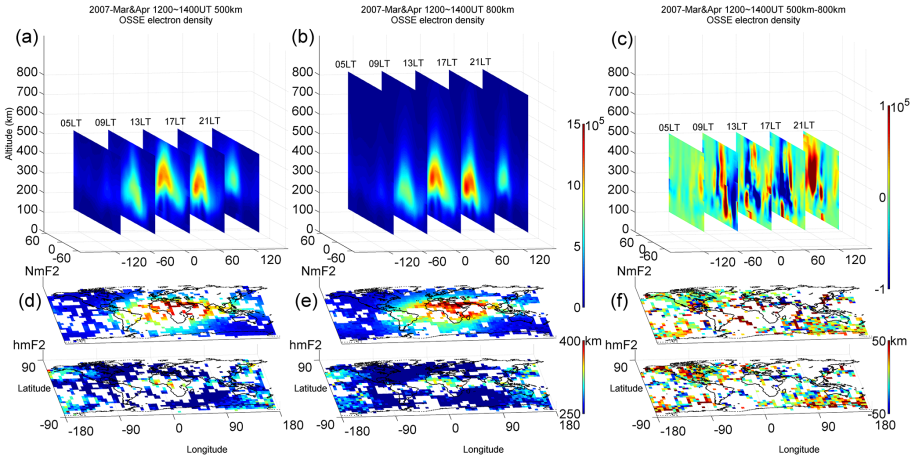

Figure 4. The Abel inversion OSSE electron density, *Nm*F2, and *hm*F2 observed from 500 and 800 km altitude satellites, and their difference during 12:00–14:00 UT in March and April 2007. **(a)** OSSE electron density observed from 500 km altitude, **(b)** OSSE electron density observed from 800 km altitude, and **(c)** their difference. **(d)** OSSE *Nm*F2 and *hm*F2 observed from 500 km altitude, **(e)** OSSE *Nm*F2 and *hm*F2 observed from 800 km altitude, and **(f)** their difference.

AMTD
8, 1615–1627, 2015

Electron density profiles probed by radio occultation

J. Y. Liu et al.

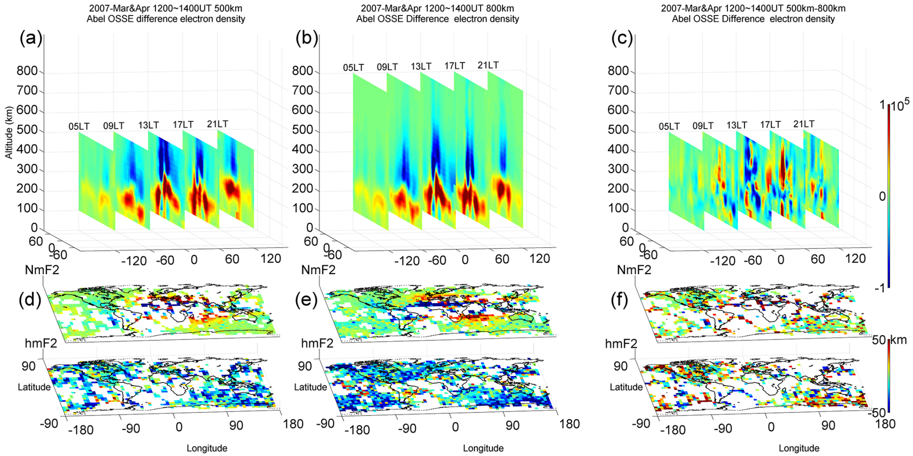

Figure 5. The Abel inversion OSSE error (OSSE result–truth) electron density, *Nm*F2, and *hm*F2 observed from 500 and 800 km altitude satellites, and their difference during 12:00–14:00 UT in March and April 2007. **(a)** OSSE electron density error observed from 500 km altitude, **(b)** OSSE electron density error observed from 800 km altitude, and **(c)** their difference. **(d)** OSSE *Nm*F2 and *hm*F2 error observed from 500 km altitude, **(e)** OSSE *Nm*F2 and *hm*F2 error observed from 800 km altitude, and **(f)** their difference.

AMTD
8, 1615–1627, 2015